21st International Conference on General relativity and Gravitation, Columbia University, New York
10–15 July 2016

Accretion of gaseous clumps from the Galactic Centre Mini-spiral onto Milky Way's supermassive black hole

Vladimir KARAS
Astronomical Institute, Prague, Czech Republic

Devaky KUNNERIATH
The North American ALMA Science Center, NRAO, Charlottesville, Virginia (VA)

Bozena CZERNY, Agata ROZANSKA, & Tek P. ADHIKARI
Nicolaus Copernicus Astronomical Centre, Warsaw, Poland

STRONGGRAVITY
EU FP7-SPACE research project 312789
2013 - 2017

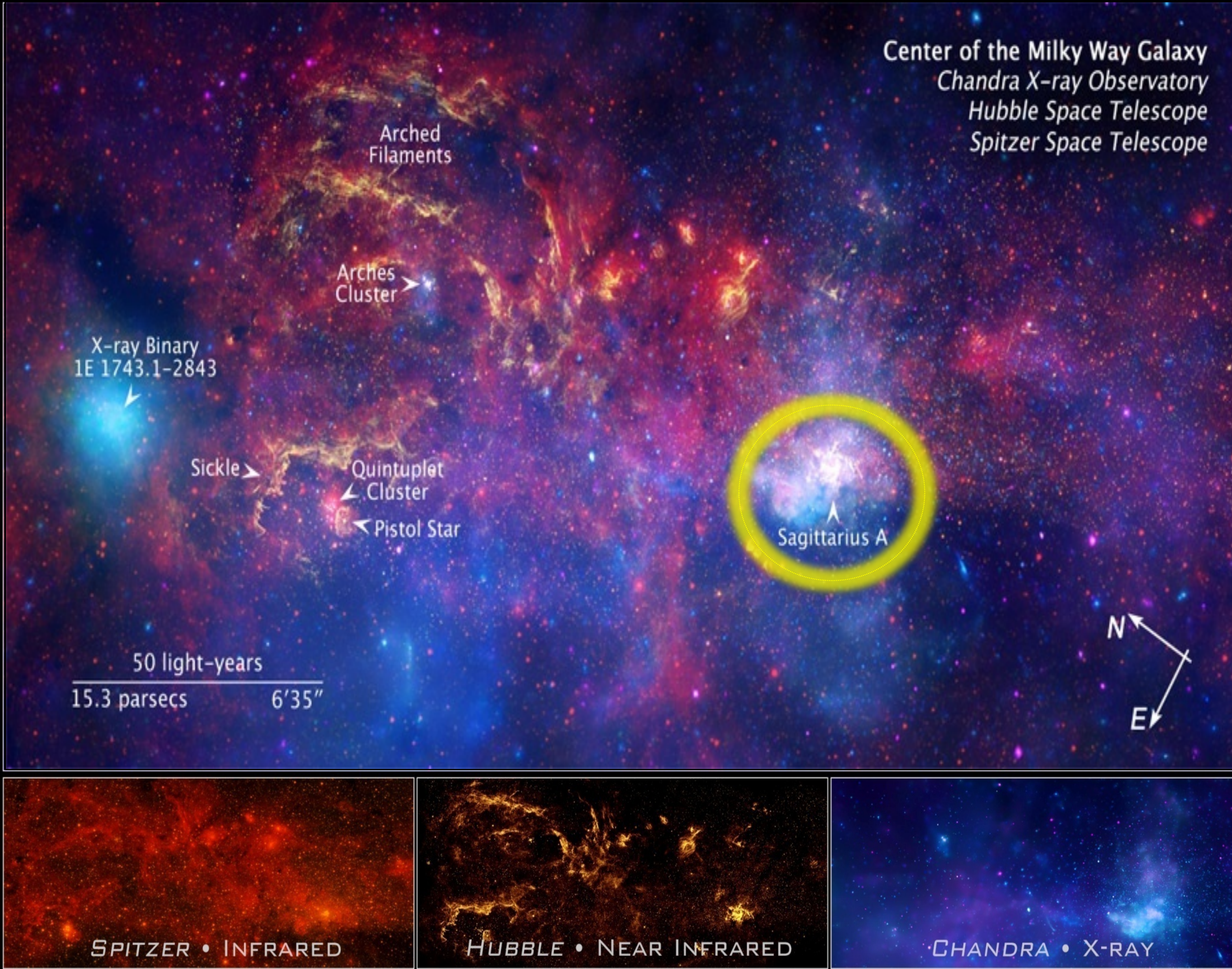
Center of the Milky Way Galaxy
Chandra X-ray Observatory
Hubble Space Telescope
Spitzer Space Telescope
Arched Filaments
Arches Cluster
X-ray Binary 1E 1743.1-2843
Sickle
Quintuplet Cluster
Pistol Star
Sagittarius A
N
E
50 light-years
15.3 parsecs
6′35″
Spitzer • Infrared
Hubble • Near Infrared
Chandra • X-ray

Artist's picture of a galactic nucleus: stars passing through gaseous environment

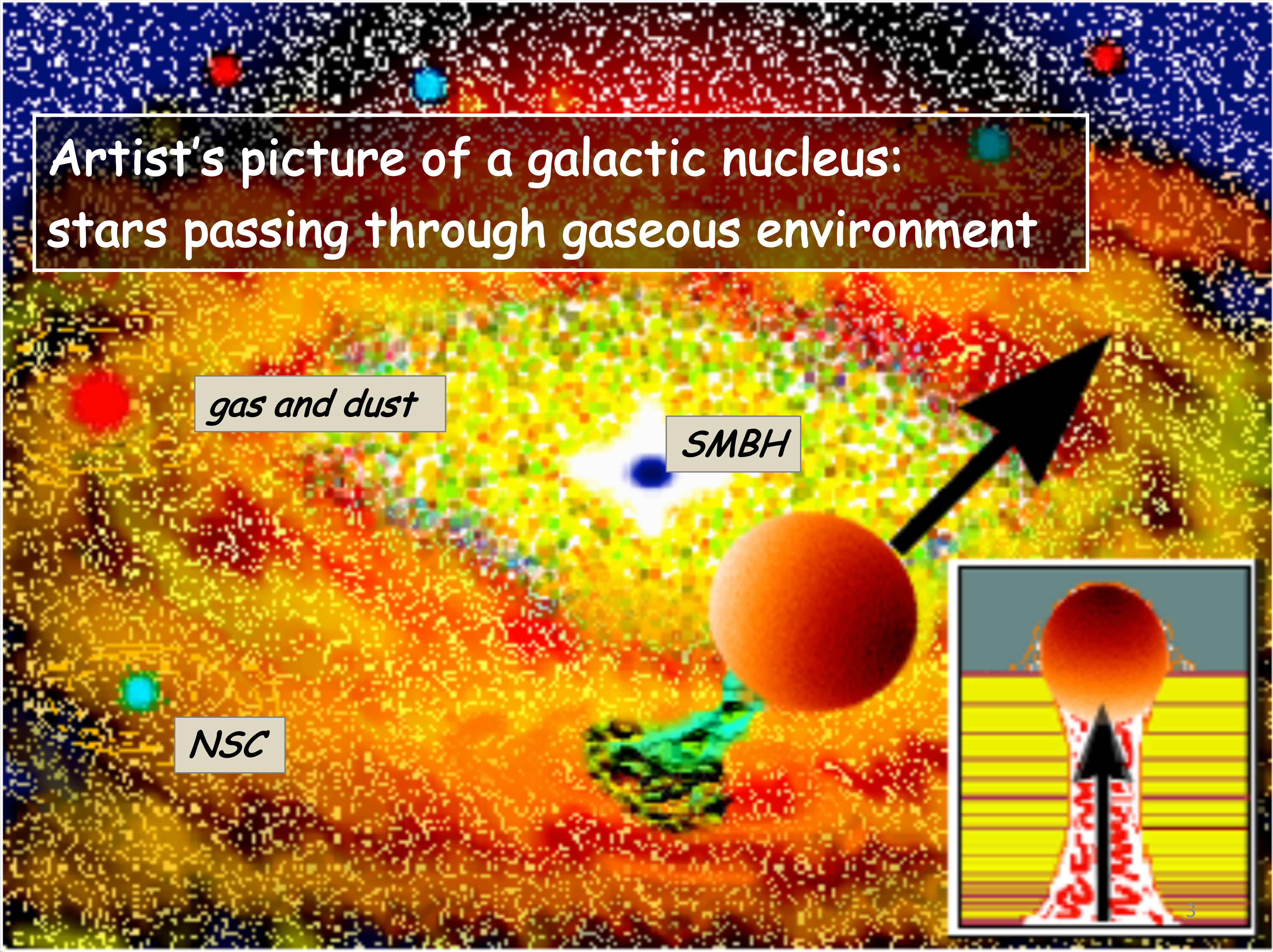

ASCA View of Our Galactic Center: Remains of Past Activities in X-Rays?

Sgr A* past activity
from its
present X-ray emission

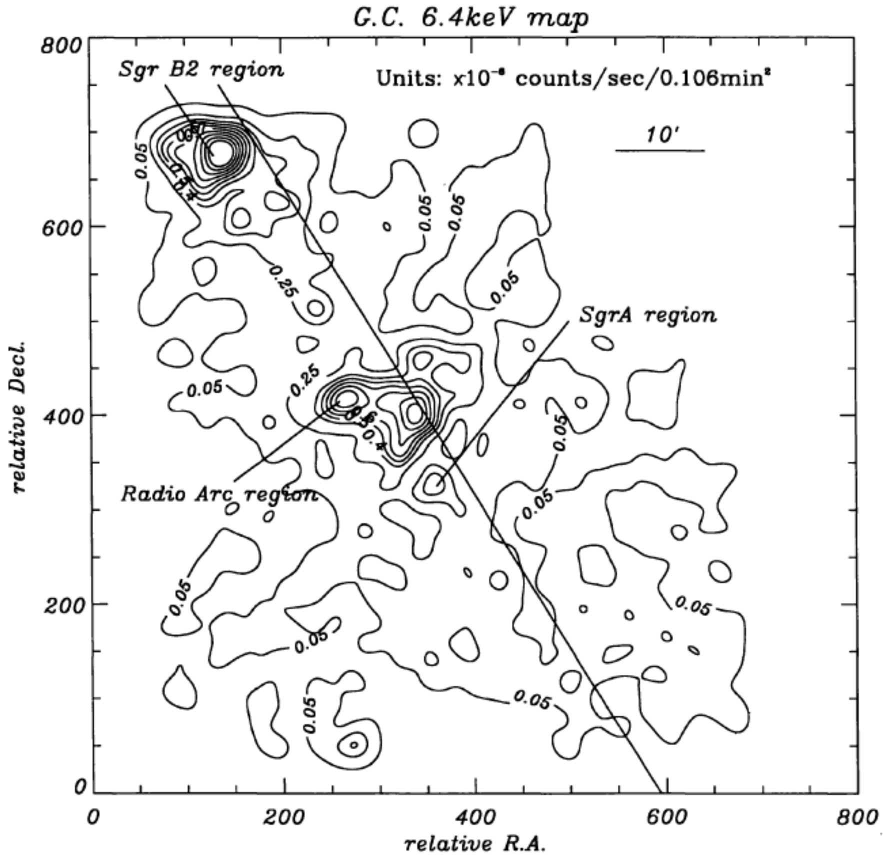

(a) Brightness distribution of the 6.4-keV line. Of the two bright regions, the northern bright spot (upper-left) is ated near to the Sgr B2 cloud; the other (middle), near the Radio Arc, appears to be associated with a recently covered molecular cloud (Lindqvist et al. 1995).

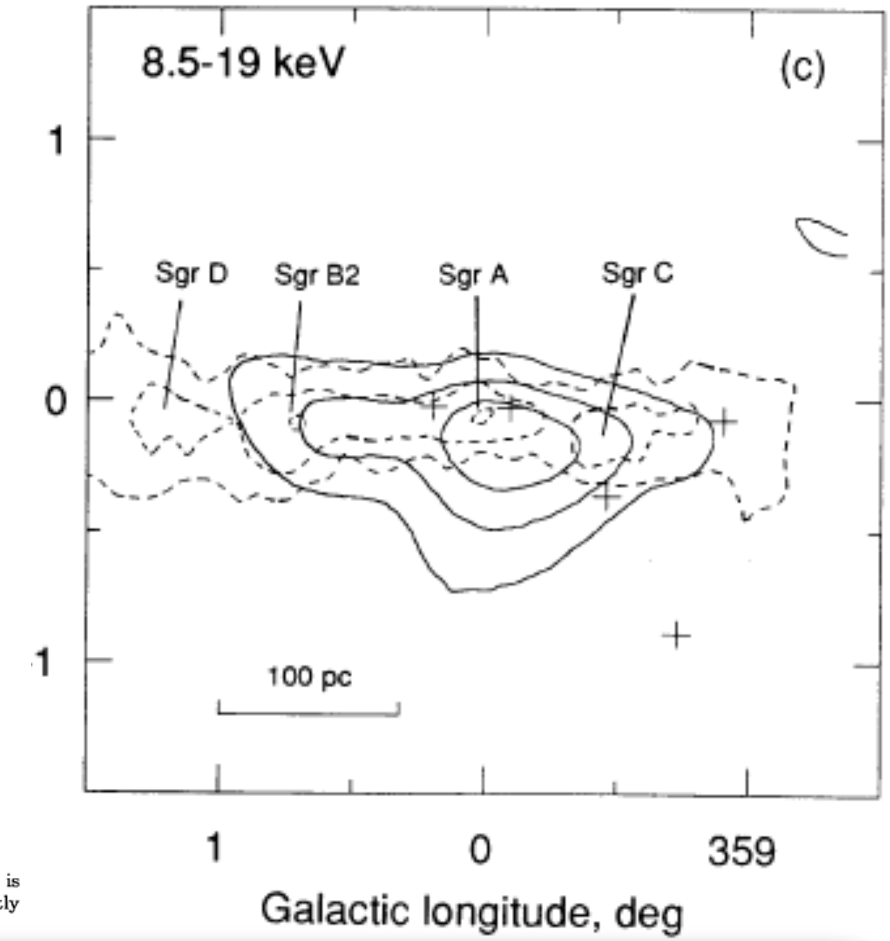

THE CENTER OF THE GALAXY IN THE RECENT PAST: A VIEW FROM *GRANAT*

Koyama et al. (1996)

Sunyaev et al. (1993)

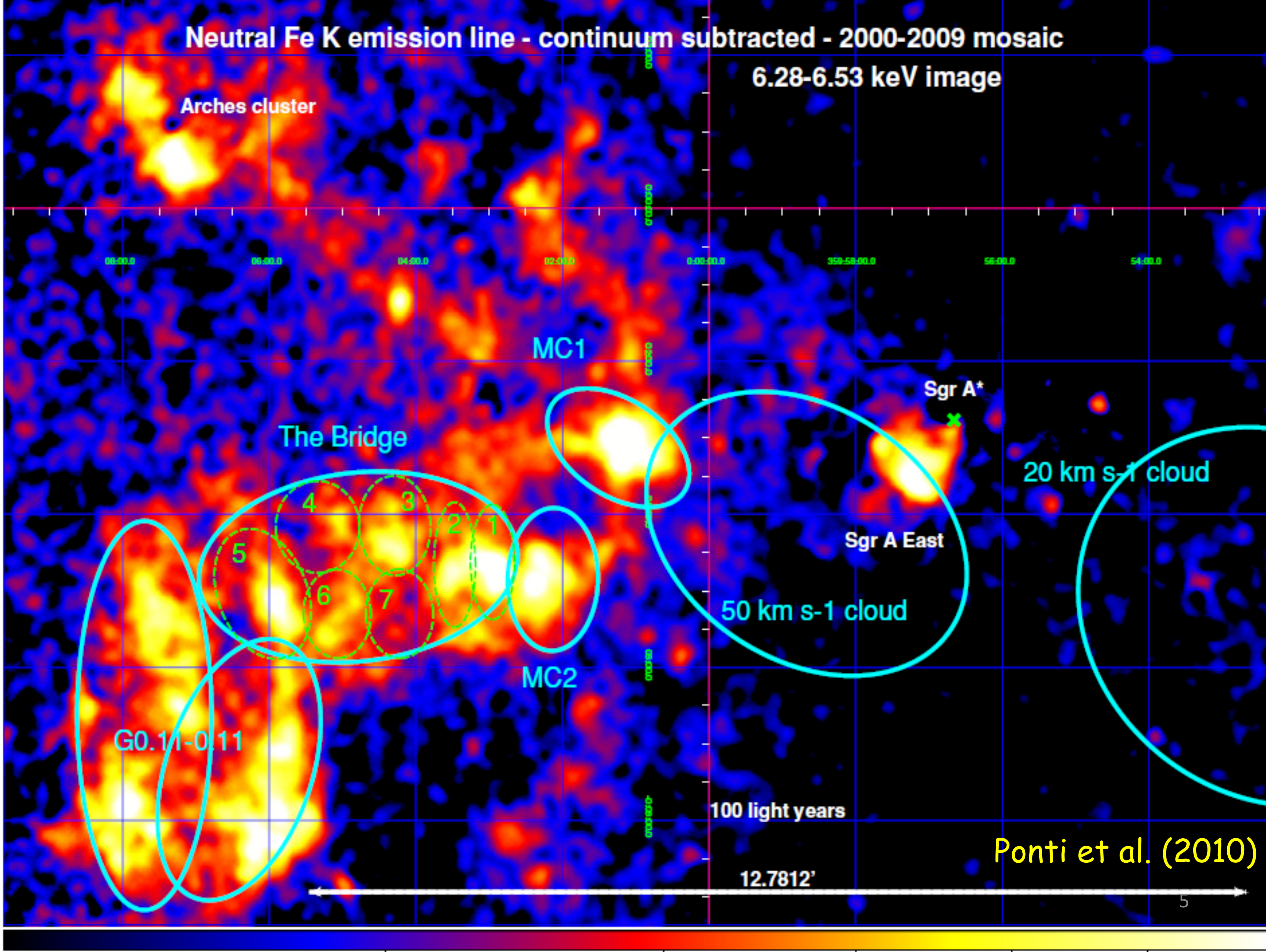

Neutral Fe K emission line - continuum subtracted - 2000-2009 mosaic
6.28-6.53 keV image
Arches cluster
MC1
Sgr A*
The Bridge
20 km s-1 cloud
Sgr A East
50 km s-1 cloud
MC2
G0.11-0.11
100 light years
12.7812'
Ponti et al. (2010)

Past activity of Sgr A* – decay of the X-ray lightcurve

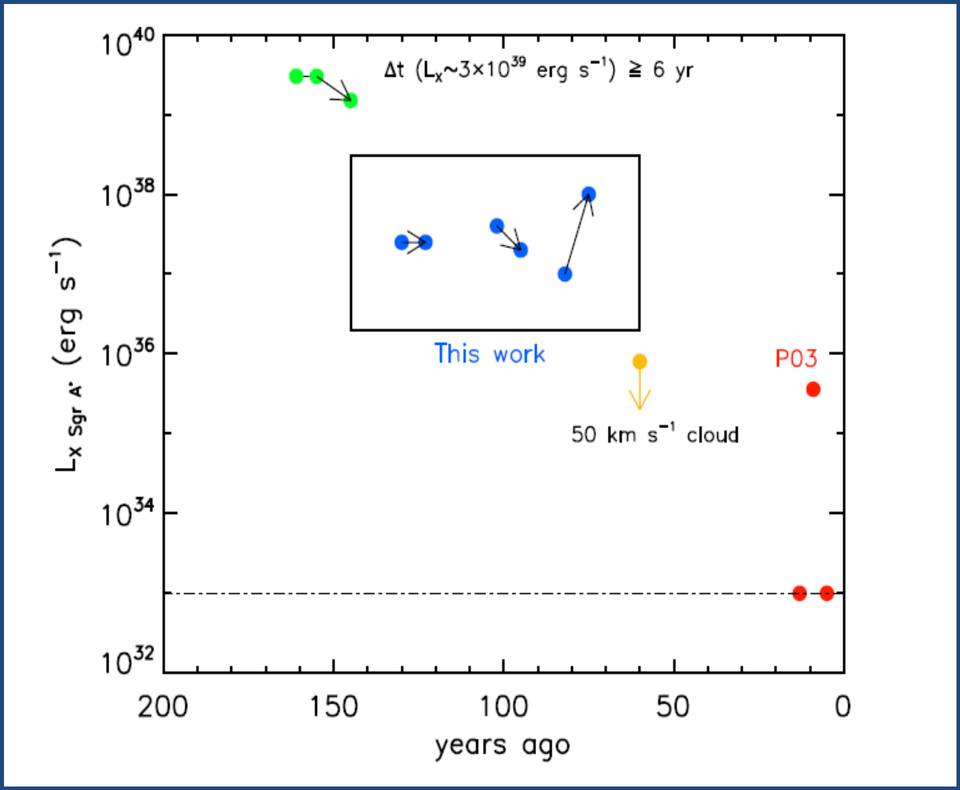

Capelli et al. (2012)

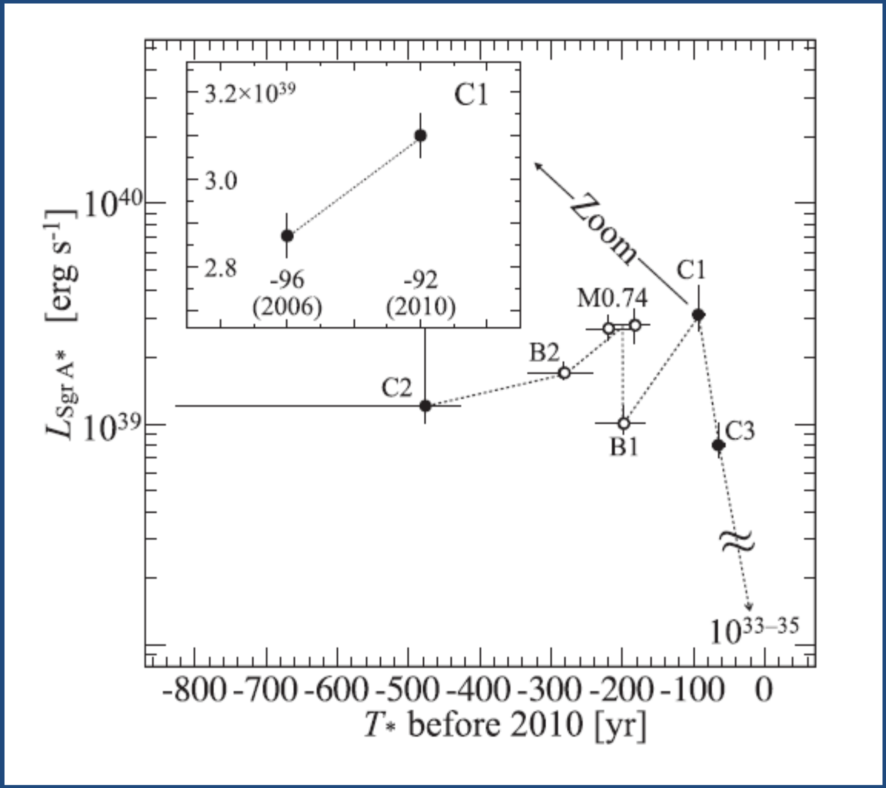

Ryu et al. (2013)

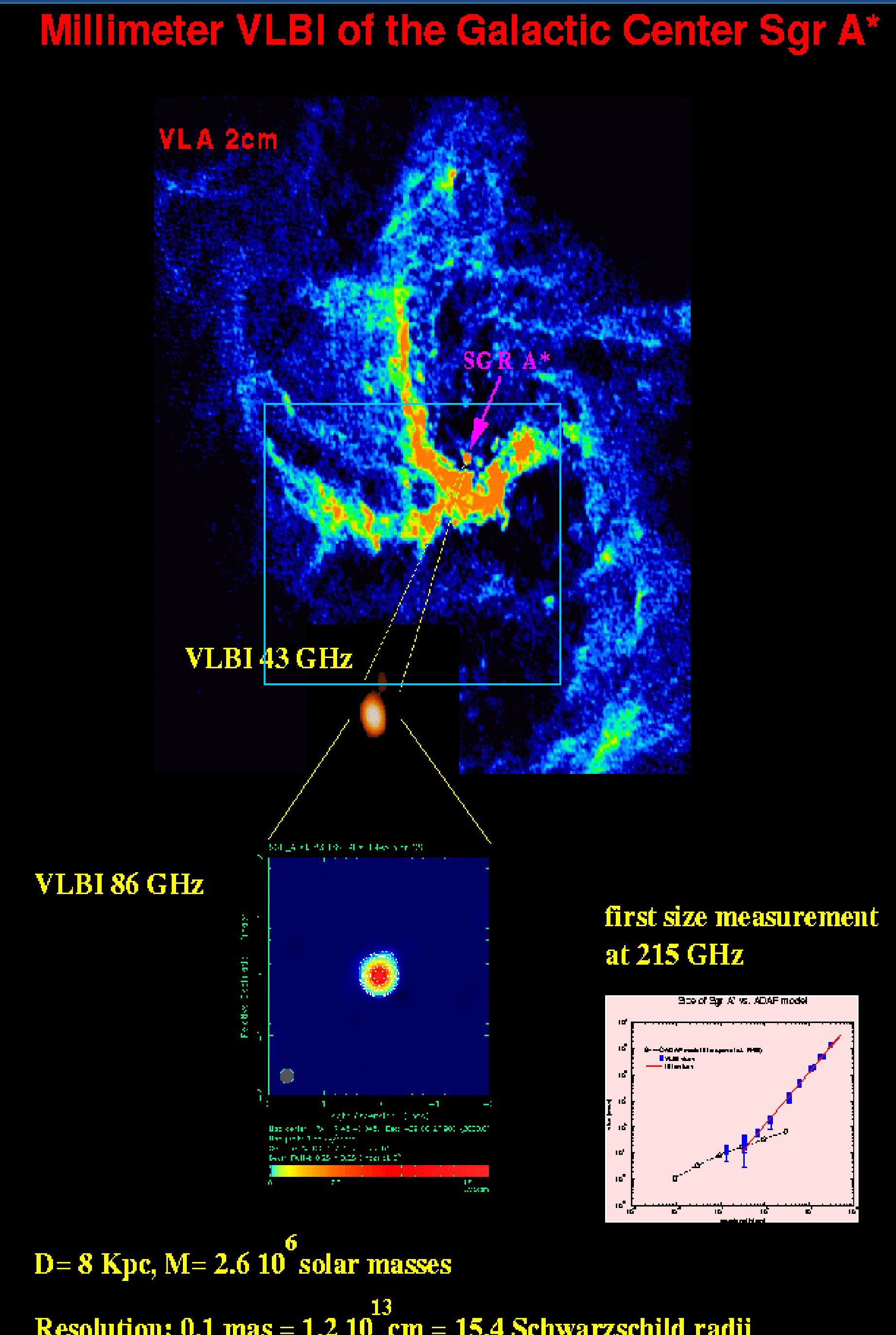

T. Krichbaum 1998

Region of interest: The Mini-spiral

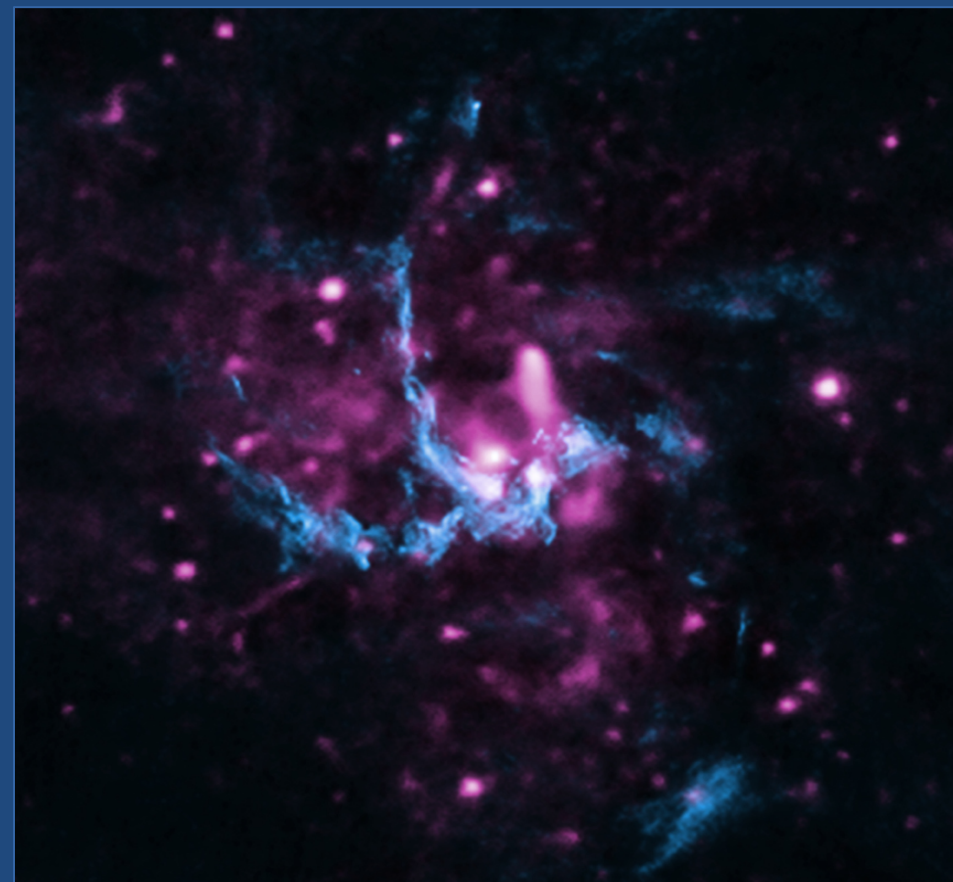

X-ray: NASA/CXC/UCLA (Li et al. 2013)
Radio: NRAO/VLA

Cold phase (gas 3-21x10^4 cm^{-3}, 5000-13000 K, and dust ~300 K)

Hot phase (fully ionised gas, n_e=18 cm^{-3}, T_e=3.5 keV at 1.5")

Region of interest: The Mini-spiral

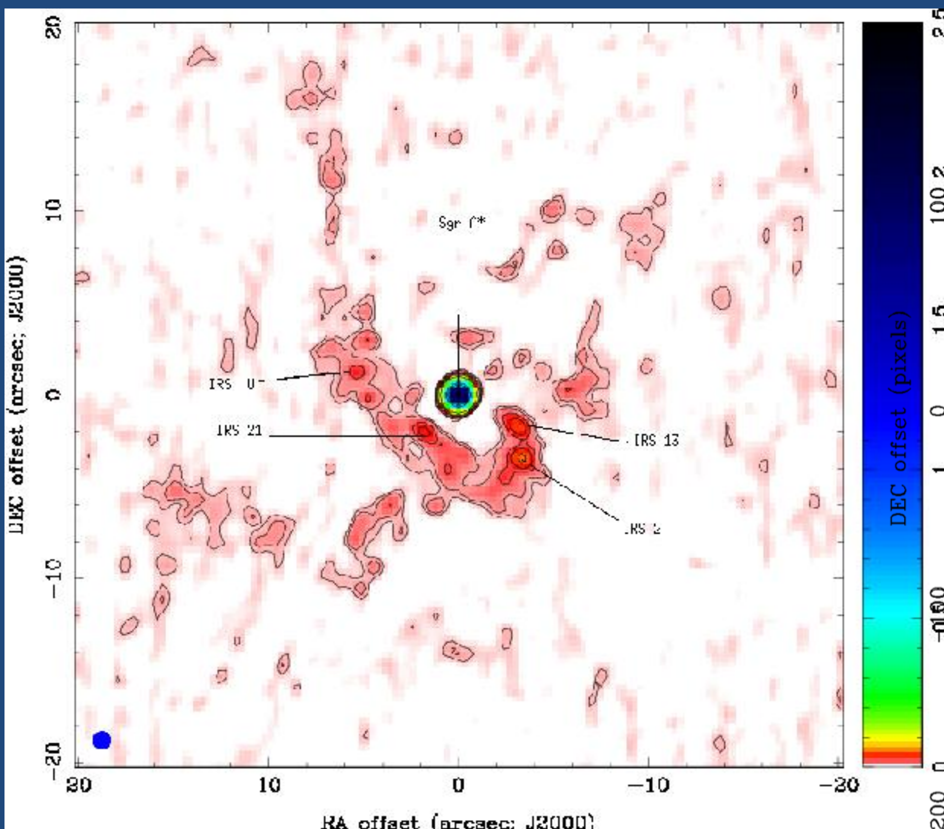

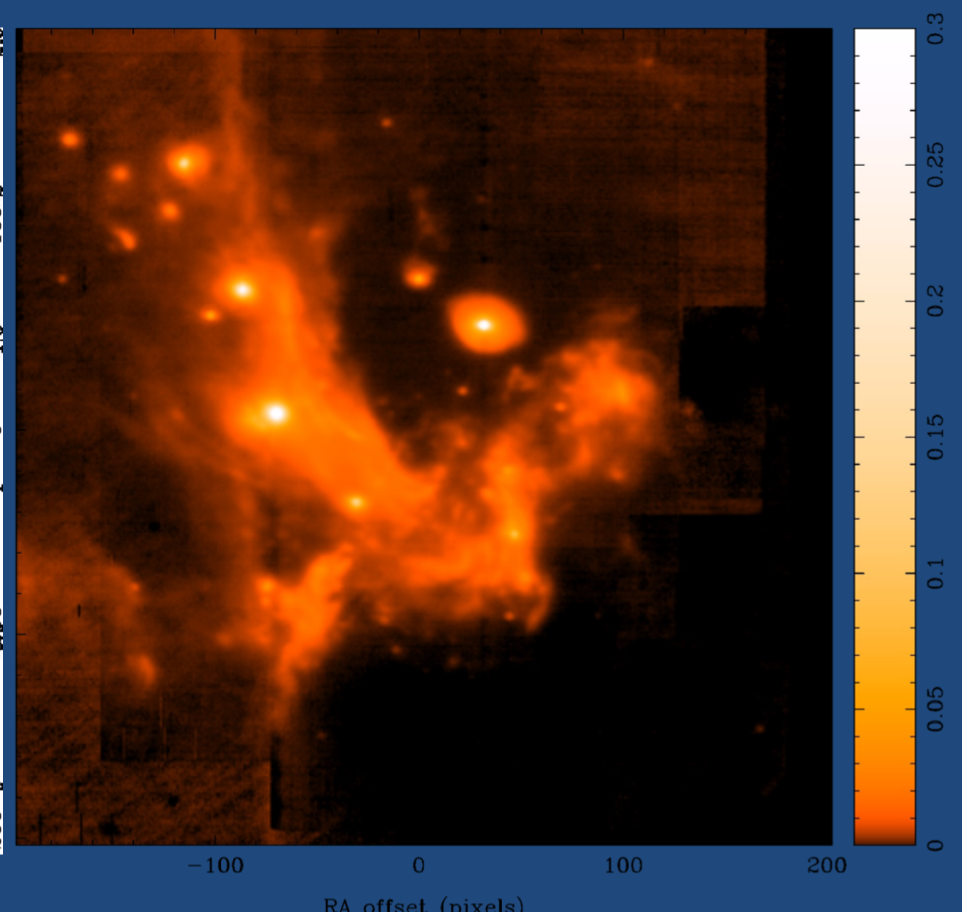

Left: radio 1.3mm (Kunneriath et al. 2012) Right: MIR 8.6 µm (Sabha et al. 2012)

Elementary accretion events from infalling clouds

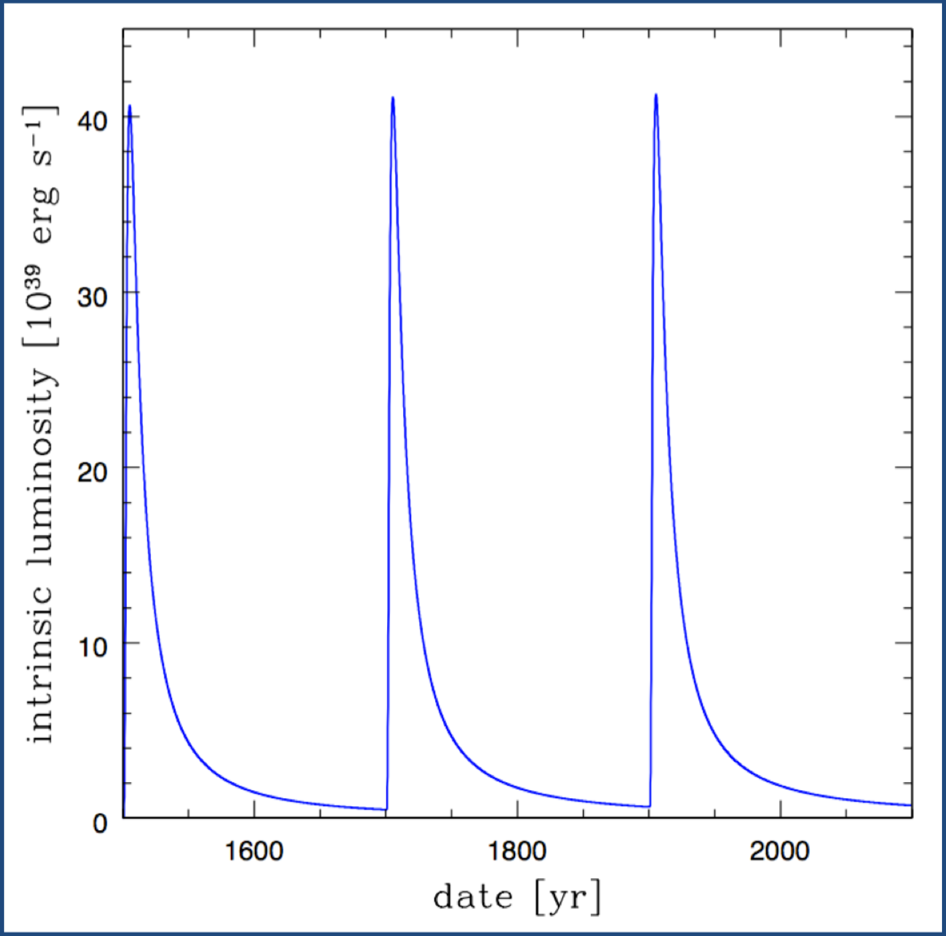

<u>'Standard' thin disk accretion:</u>

$dM/dt_{|(R)} \sim 6\pi R^{1/2}\,\delta(R^{1/2}\,\nu\Sigma)\,/\,\delta R$

(Lynden-Bell & Pringle 1974)

<u>Superposition of elementary events:</u>

$dM/dt_{|(0)} \sim t^{-5/3} / t_{visc}$

(Zdziarski et al. 2009)

Multiple accretion events

Past activity of Sgr A*

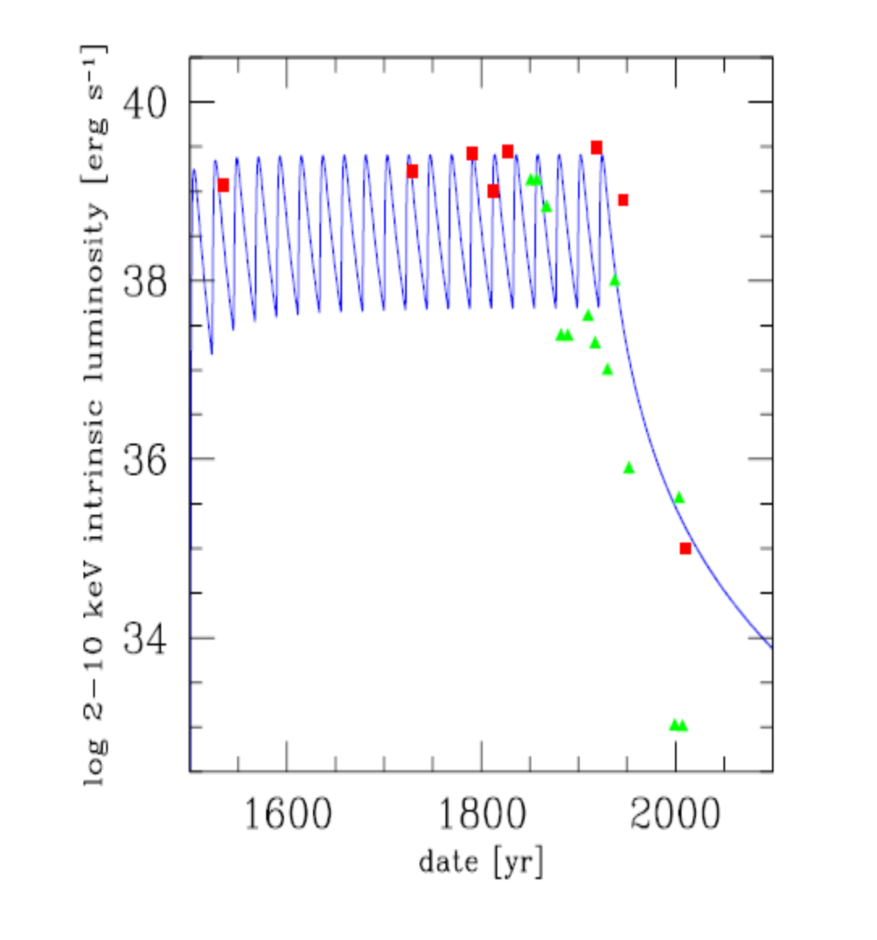

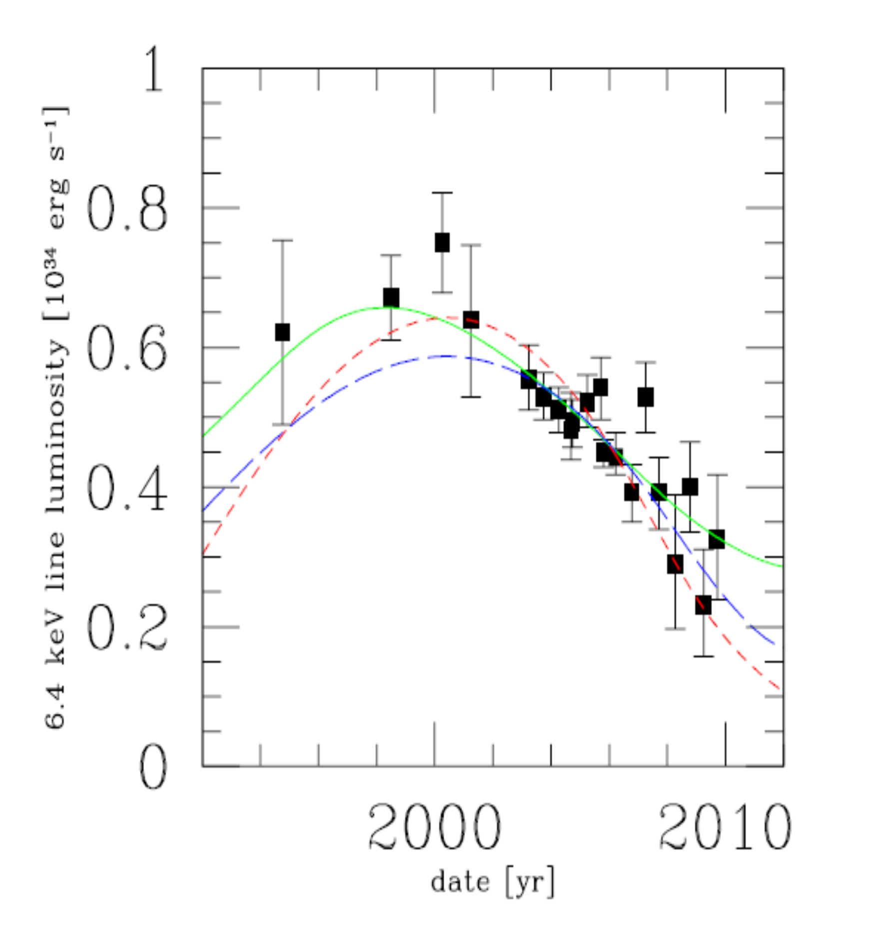

(Czerny et al. 2013)

…to study accretion driven by the *thermal instability* (TI)

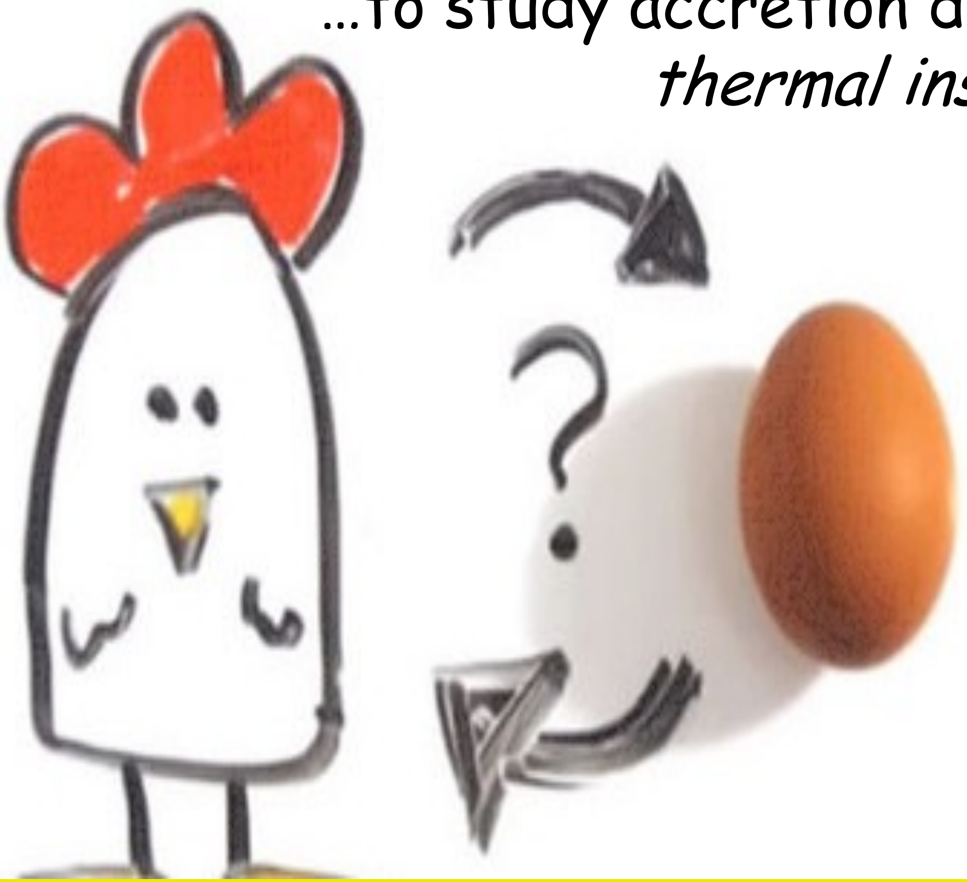

Triggering the accretion events: thermal instability in a two-phase medium

• **Field (1965)** – Radiatively heated plasma can be thermally unstable (cooler, dense matter coexists with hot medium in pressure equilibrium)

λ_F = mean thermal conduction / total heating per volume → $(10^{-7}T^{7/2} / H_{tot})^{1/2}$

Clumps of size < λ_F **evaporate**

• **Barai et al (2012)** – Two-phase medium forms spontaneously.

Ionization parameter:

$\Xi = P_{rad} / P_{gas}$ → $(L_{central} + L_{stars}) / (P_{gas} c R^2)$

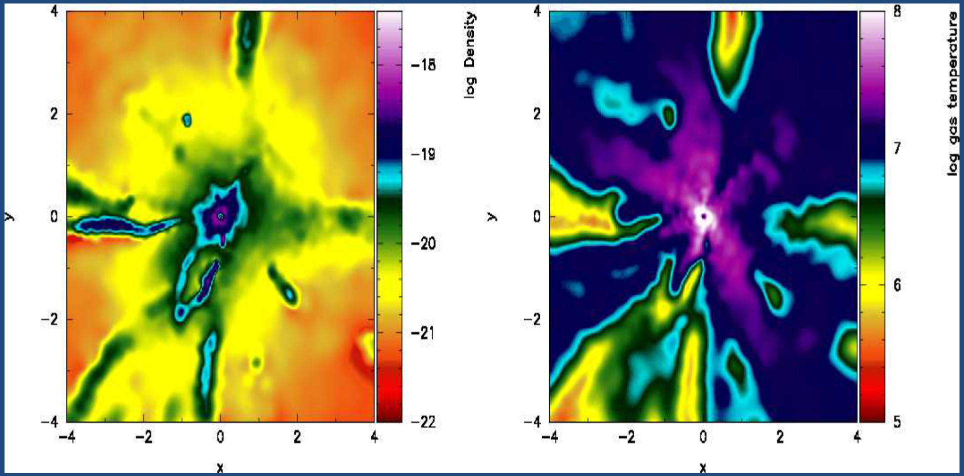

• **Moscibrodzka et al (2013): filaments break into cloudlets**

Cooling time:

$t_{cool} \sim E / L_{tot}$, $L_{tot} \sim n^2 T^{1/2}$

Colder clumps form filaments → they become accreted faster → **enhanced accretion rate**

Method and parameters

Cloudy photoionisation code to model the ISM in the GC

- calculate instability curves log(T) vs. log(Ξ) for different luminosity states of Sgr A*,
- include the influence of *dust grains* on the onset of TI
- include the influence of *stellar radiation and winds*.

We consider

- clouds: different density and different distance
- accretion mode: $M_{dot} \sim m \times 10^{-9}\ M_{sun}\ yr^{-1}$

Thermal instability – different states of luminosity (distance R=0.008pc from the center)

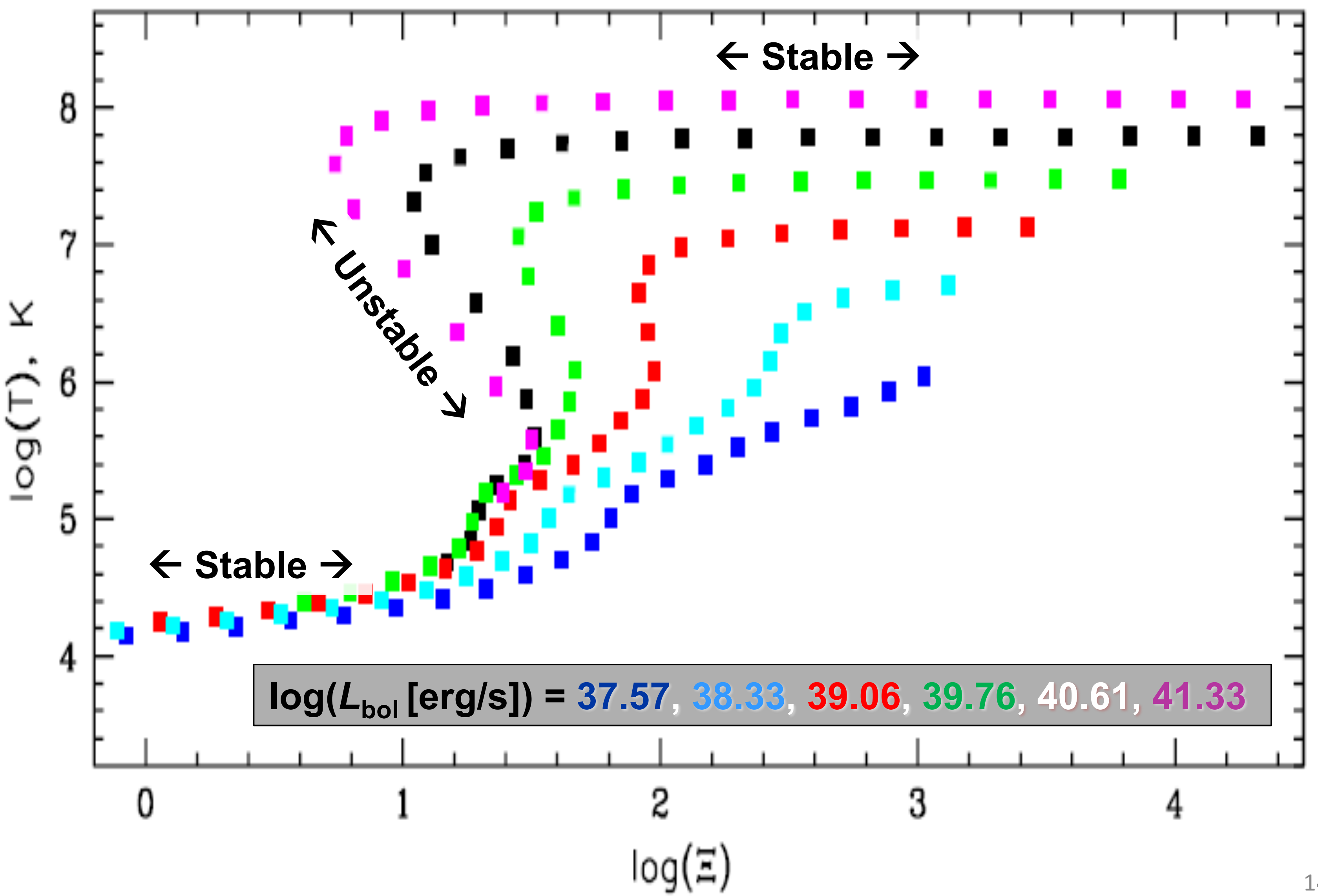

Thermal instability for different states of luminosity (R=0.008pc)

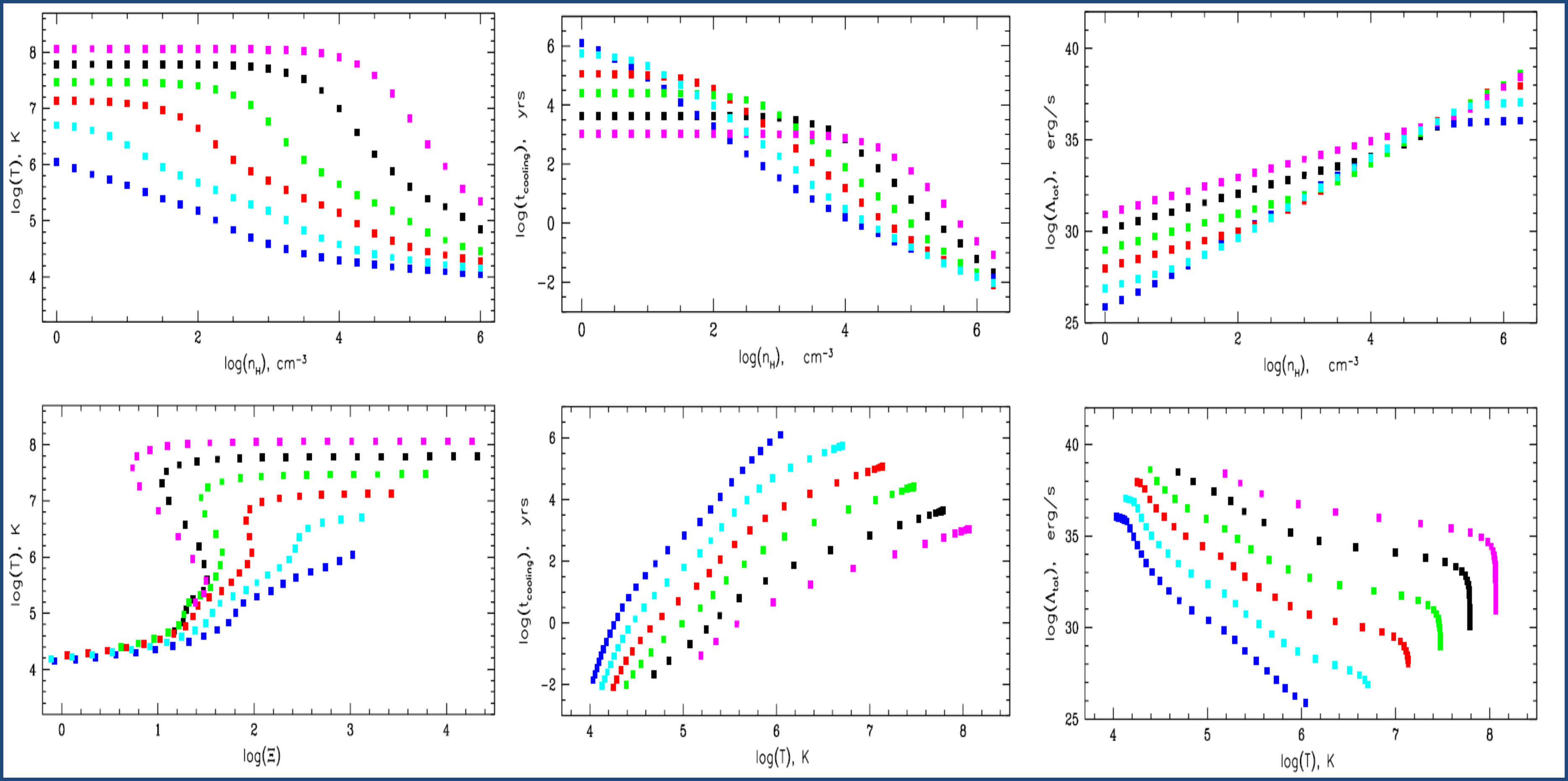

log(L_{bol} [erg/s]) = 37.57, 38.33, 39.06, 39.76, 40.61, 41.33

Influence of dust: suppression of instability

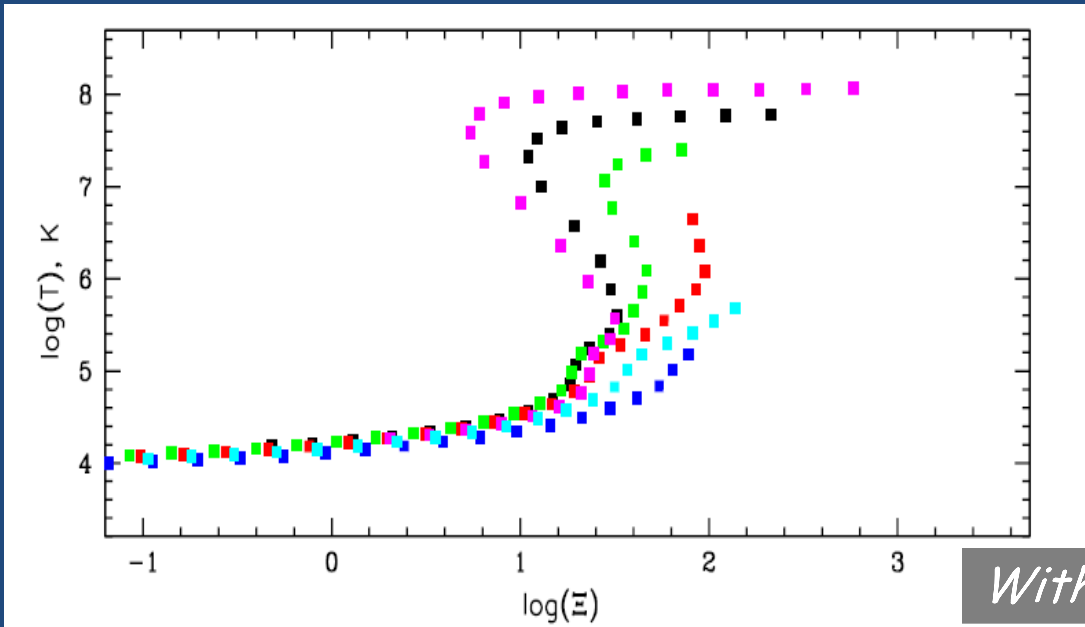

Without dust

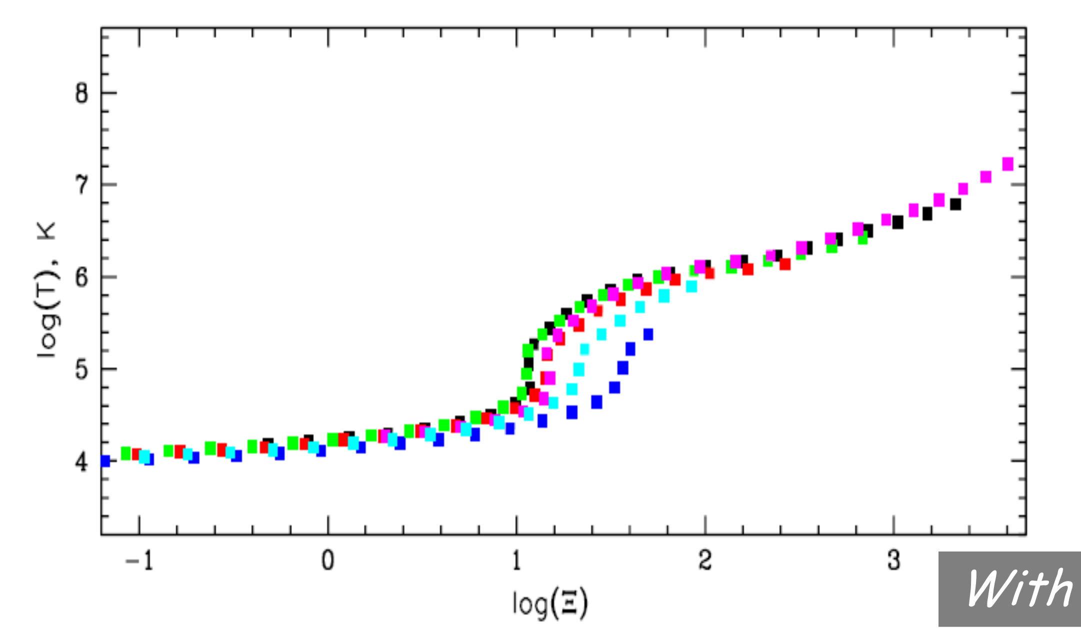

With dust: suppresing the instability

The Mini-spiral contains dust (200–300K; Cotera et al. 1999).

(Treated by an option in Cloudy.)

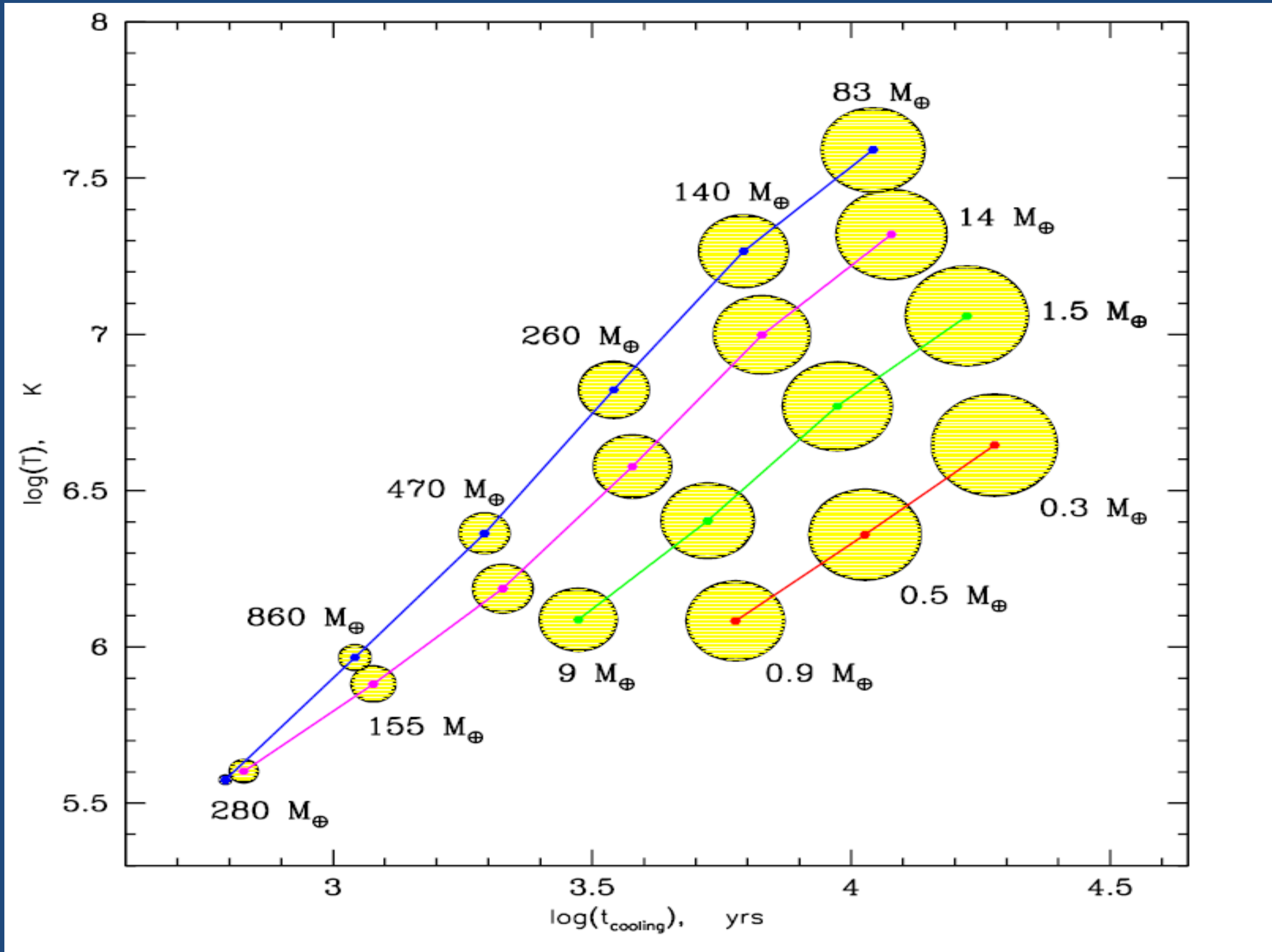

Size of clouds

Thermal conduction limits the smallest size of the clouds
(Rozanska et al. 2014).

- Four different curves: bolometric luminosity L_{bol}
- Radius of the yellow circles: Field length λ_F
- Mass of clouds M_c in units of Earth mass

Instability strips for two-phase medium within Bondi flow

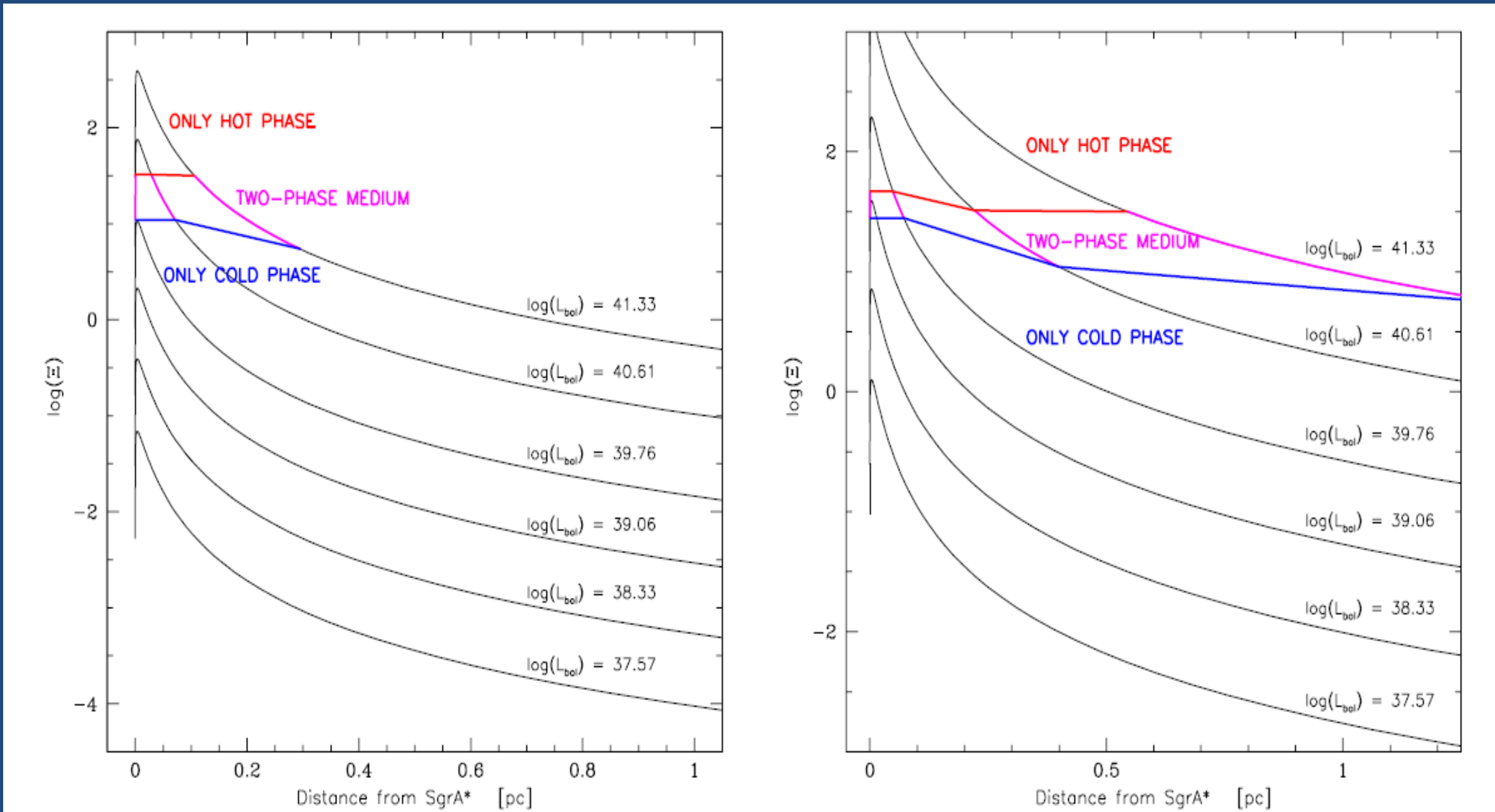

n_{out} = 18 cm^{-3} n_{out} = 1 cm^{-3}

The role of stellar radiation and wind (mechanical heating)

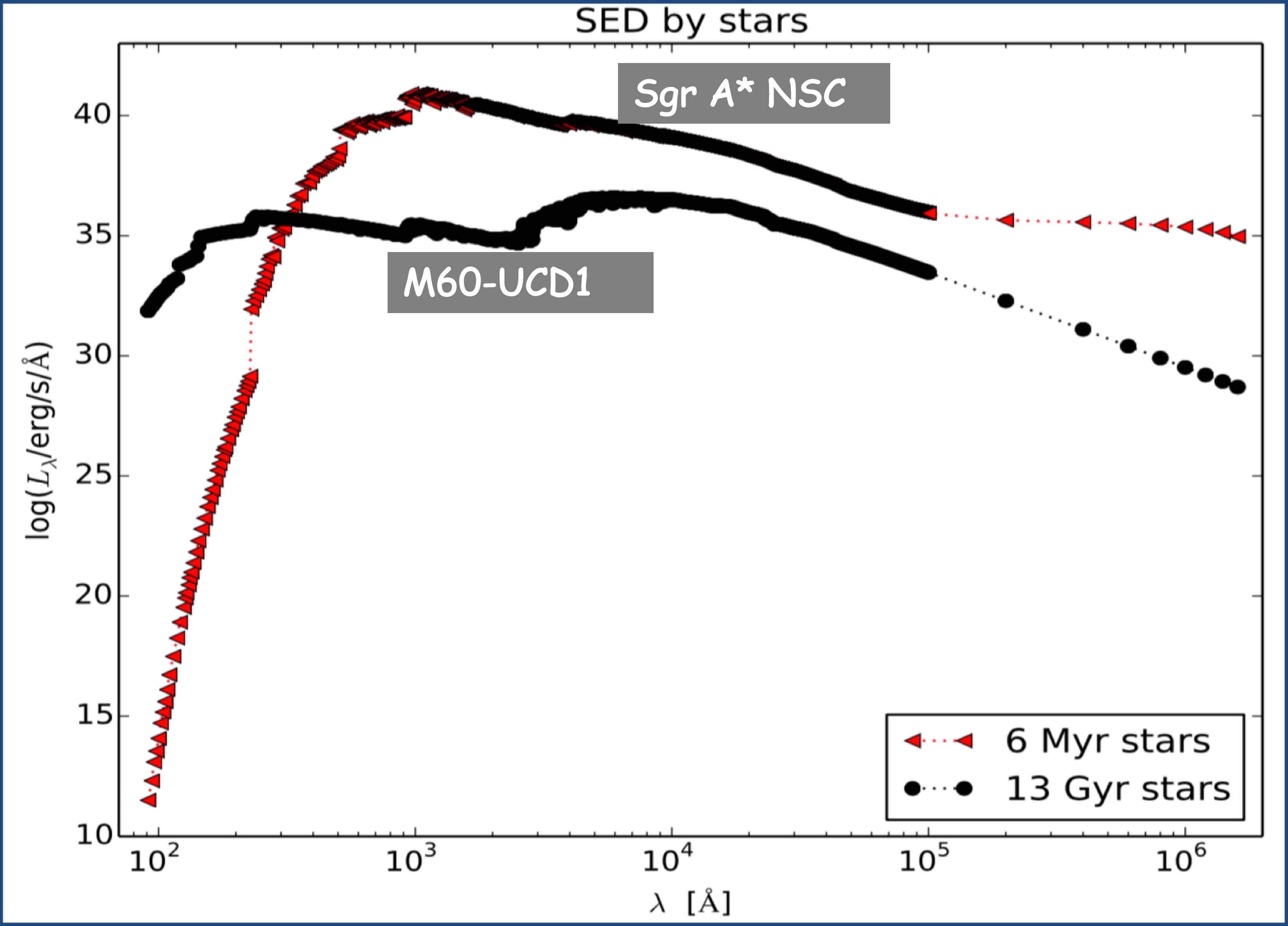

S-curves of Thermal Instability: Temperature vs. Ionisation parameter

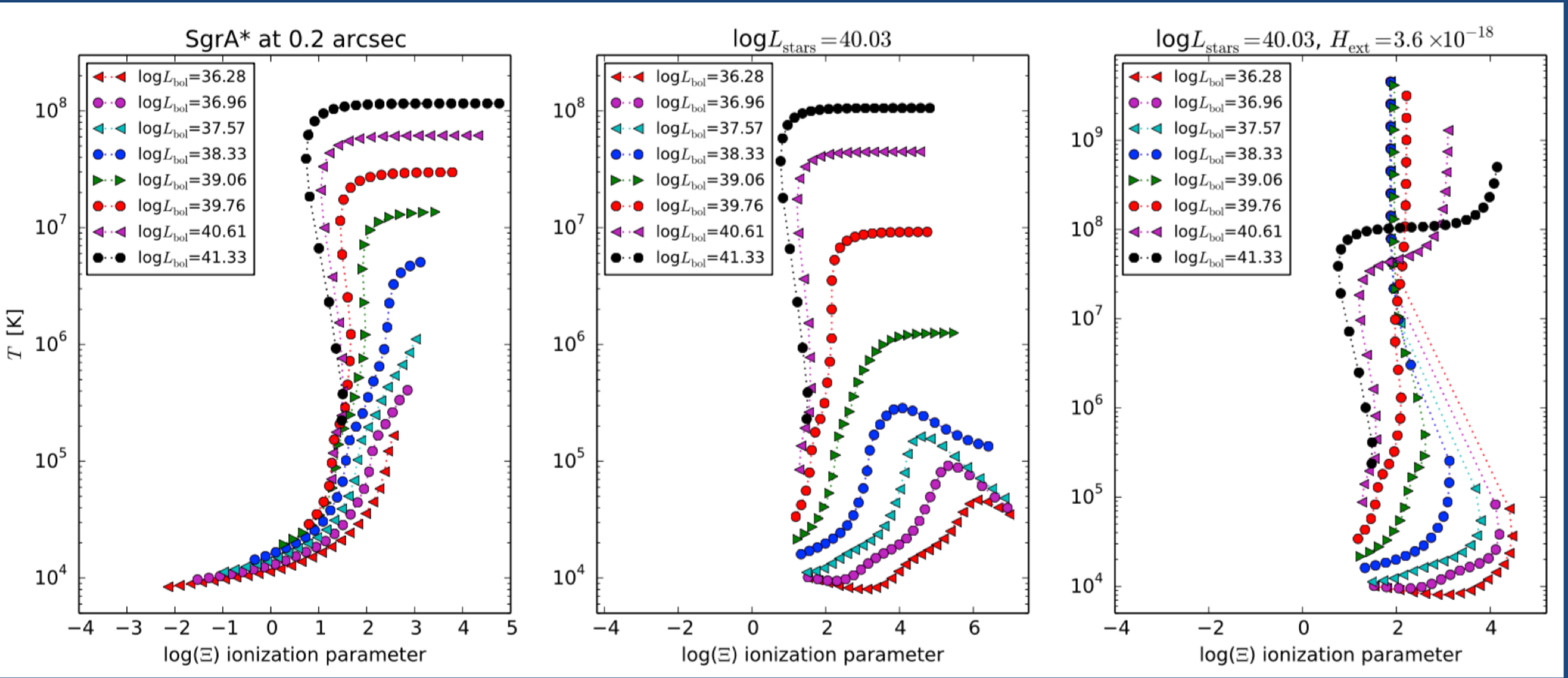

Only the central source of irradiation → + Including the stellar radiation by 6 Myr SED → + Including the stellar mechanical heating by winds

Conclusions

- Current level of luminosity of Sgr A* *not enough* to drive the thermal instability

- For luminosity > 10^{39} erg/s at distance ~ 0.008–0.2 pc, the thermal instability operates, *cold clumps can accrete*

- Cooling time-scales are long (~ hundreds years)

- Typical cloud size of 10^{14-15} cm, mass of ~10 M_{Earth}

- Influence of dust is small

Thank you!

Discussion slides:
Two-phase medium in Bondi flow around Sgr A*

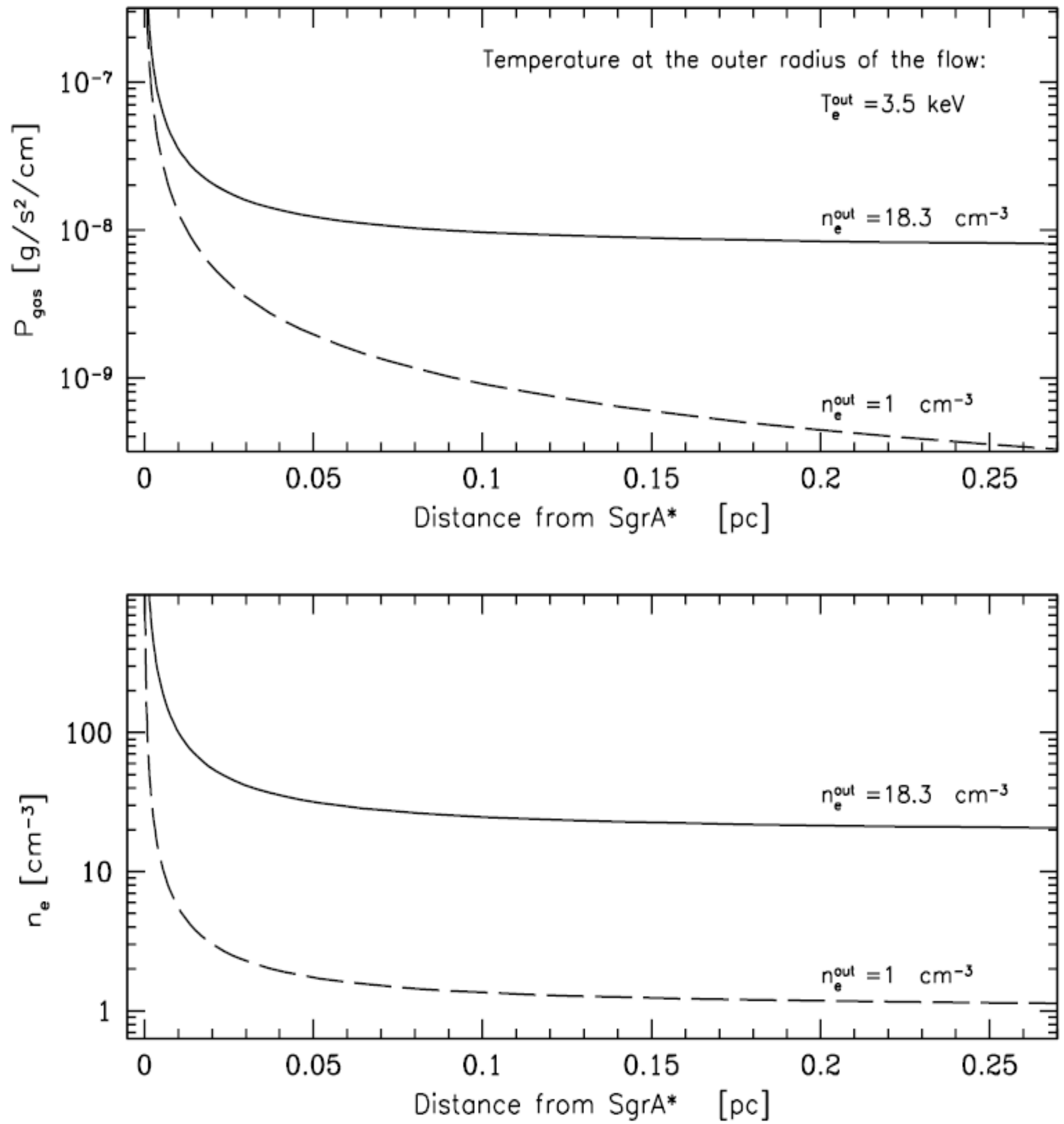

Bondi accretion operates up to ~ 0.1pc from Sgr A*

Thermal instability for different states of luminosity (R=0.2pc)

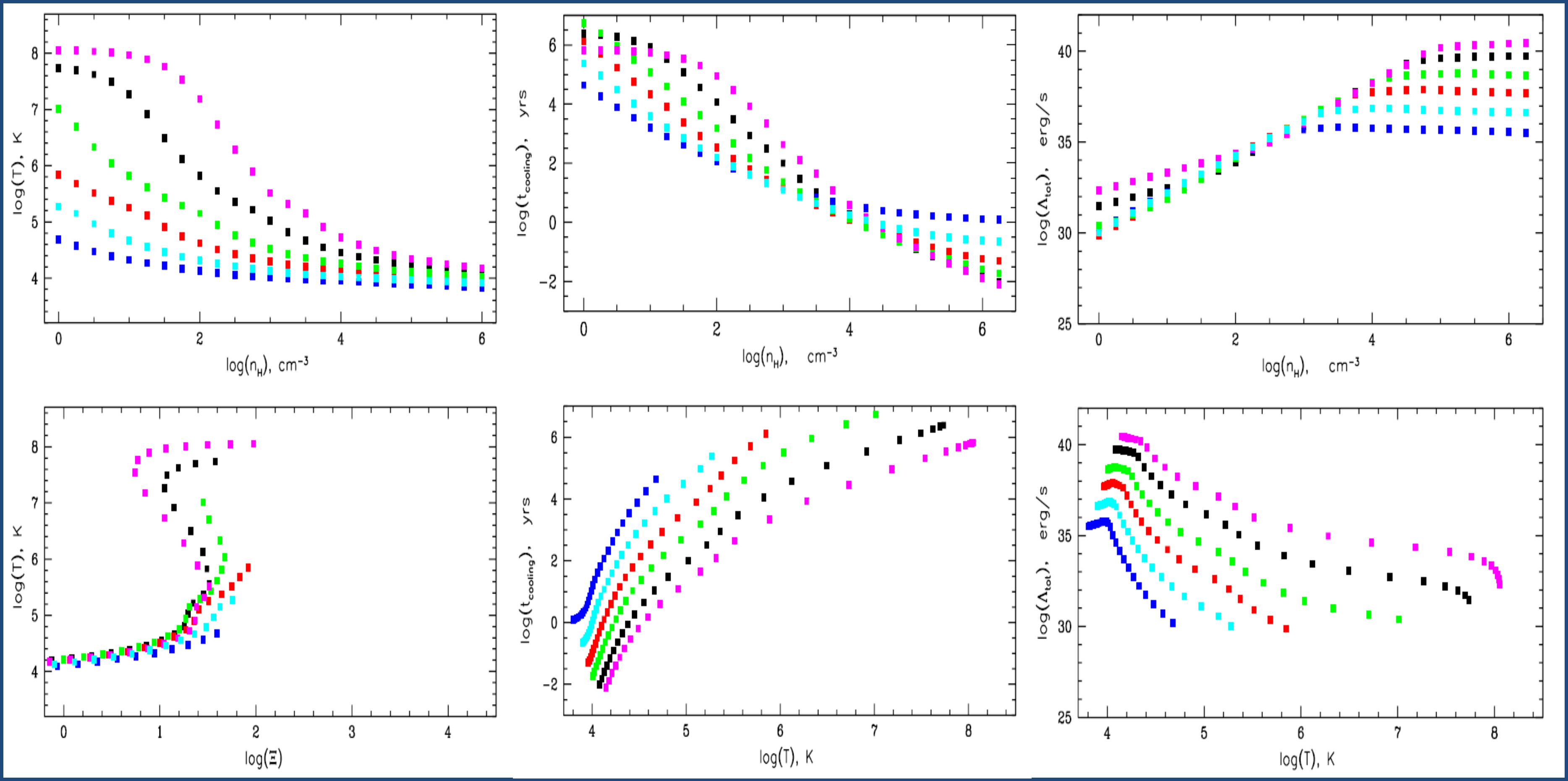

$\log(L_{bol}$ [erg/s]) = 37.57, 38.33, 39.06, 39.76, 40.61, 41.33

Past activity of Sgr A* – predictions for X-ray polarimetry

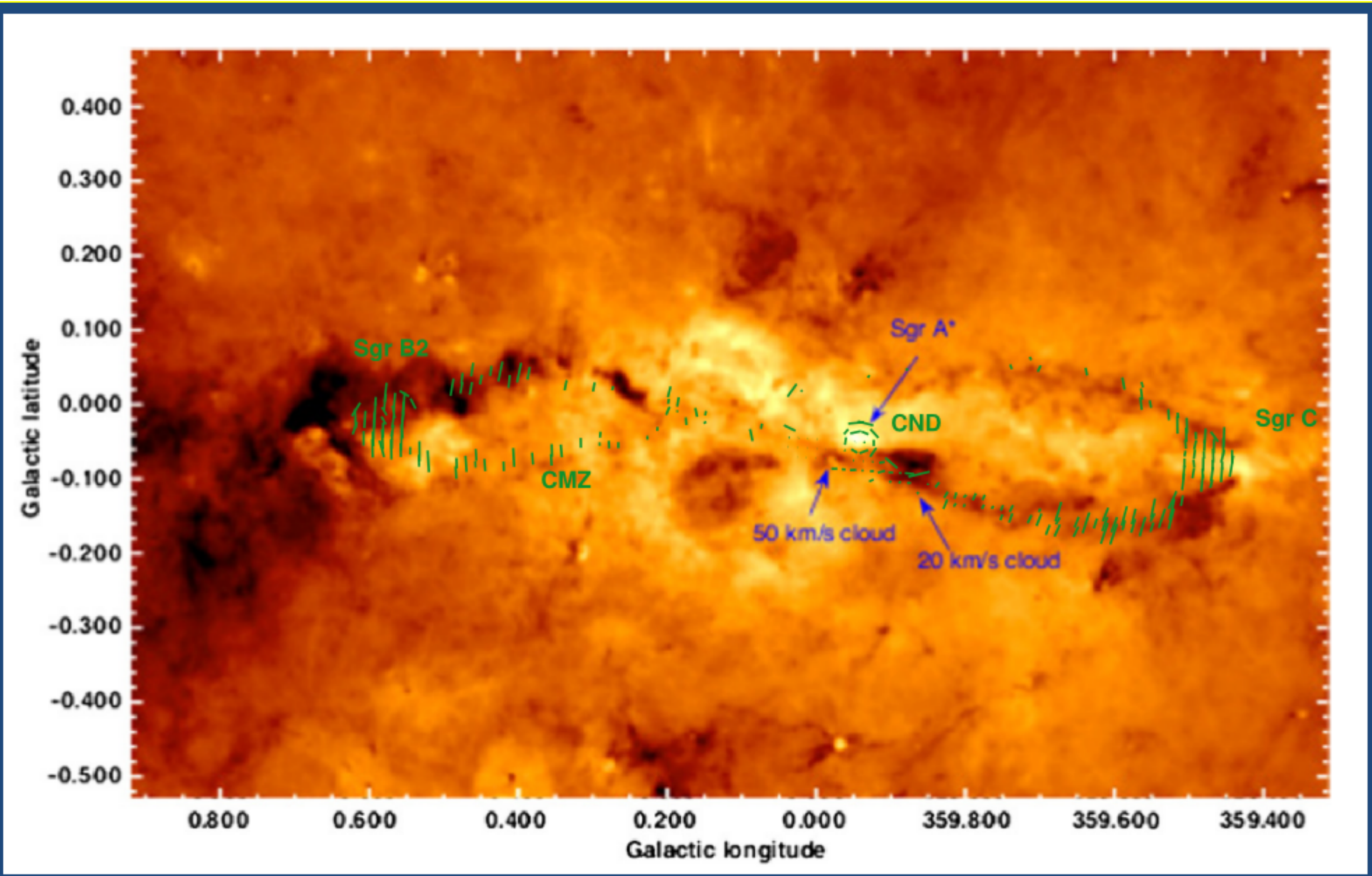

Molinari et al. (2011), Marin et al. (2014)

Past activity of Sgr A* – predictions for X-ray polarimetry

Table 1. Parameterization of the reflection nebulae, modeled with uniform-density, spherical clouds filled with cold, solar abundance matter.

Molecular cloud	Cloud radius (pc)	Projected distance[a] (pc)	Line of sight distance[b] (pc)	Offset[c] (pc)	Velocity[d] ($km\,s^{-1}$)	Hydrogen column density ($\times 10^{22}$ cm^{-2})	Electron optical depth	References
Sgr B2	5	–100	–17	–4.0	60	80	0.5	E, I
Sgr B1	6	–79.1	–23	–6	–45	12.3	0.3	A, D, G
G0.11-0.11	3.7	–25	–17	–13	25	2	0.03	E, F
Bridge E	2.0	–21.6	–60	–1.3	55	9.6	0.07	B, E, F
Bridge D	1.6	–18.3	–60	0.5	55	13.2	0.09	B, E, F
Bridge B2	1.8	–16.3	–60	–1.5	55	12.3	0.08	B, E, F
MC2	1.8	–14	<–17	–2.6	–10	<2	0.36	C, E
MC1	1.8	–12	–50	1.3	–15	4	0.32	E
Sgr C3	6	50	–53	–12	60	8.7	<1	H, E
Sgr C2	4.7	66	58	–14	60	11.4	<1	H, E
Sgr C1	4.7	71	–74	–1.5	60	6.5	<1	H, E

Notes. [(a)] Positive = east of the Galactic center; [(b)] Positive = behind the Galactic plane (farther to us than Sgr A*); [(c)] Positive = above the equatorial plane. [(d)] Positive = away from Earth.

References. A: An et al. (2013); B: Capelli et al. (2012); C: Clavel et al. (2013); D: Downes et al. (1980); E: Ponti et al. (2010); F: Ponti et al. (2014); G: Ryu et al. (2009); H: Ryu et al. (2013) and I: Sunyaev et al. (1993).

Marin et al. (2015)

Past activity of Sgr A* – predictions for X-ray polarimetry

Table 2. Integrated 4–8 keV polarization degree P o ref n component (including neutral iron lines) and polarization position angle ψ of the GC molecular clouds from the simulation with ES.

Molecular cloud	P (%)	ψ (°)	f_R (%)	$P_{exp.}$ (%)	$P_{detect.}$ (%)	$\psi_{detect.}$ (°)
Sgr B2	65.0	88.3	70.0	45.5	57.4 ± 4.4	83.3 ± 3.4
Sgr B1	76.9	84.4	52.6	40.5	40.4 ± 3.9	80.3 ± 3.3
G0.11-0.11	55.8	61.6	–	–	–	–
Bridge E	12.7	67.9	–	–	–	–
Bridge D	0.1	74.2	–	–	–	–
Bridge B2	15.8	77.8	–	–	–	–
MC2	25.8	73.8	–	–	–	–
MC1	0.1	77.5	–	–	–	–
Sgr C3	32.9	106.4	50.7	16.7	15.5 ± 2.4	109.0 ± 4.5
Sgr C2	34.9	99.1	63.0	22.0	17.9 ± 3.8	99.1 ± 5.6
Sgr C1	31.1	94.6	60.2	18.7	23.1 ± 3.3	98.1 ± 6.0

Notes. Polarization angles are defined with respect to Galactic north, with positive defined as west to north. The fraction of the total flux that is reflected f_R is computed from Ryu et al. (2009, 2013), allowing us to evaluate the diluted polarization signal $P_{exp.}$. Using Monte Carlo simulations associated with the GPD instrument (see text), we finally show estimations of the polarization degree $P_{detect.}$ and angle $\psi_{detect.}$ that a future polarimeter would detect. The empty cells correspond to clouds with too low X-ray luminosities to be observed within 3 Ms or with unestimated fractions of the reflected flux.

Marin et al. (2015)

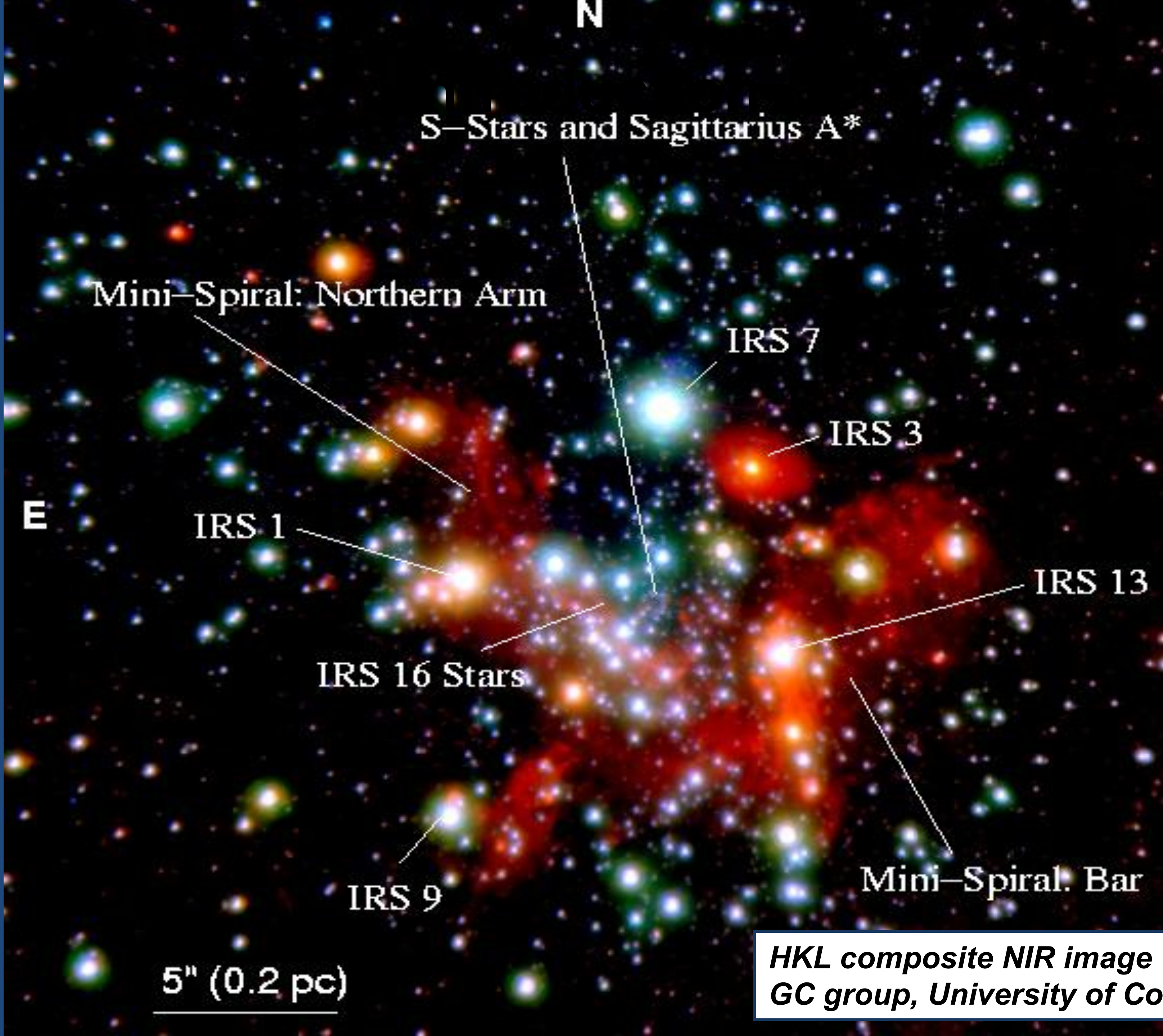

HKL composite NIR image
GC group, University of Cologne